

Stepwise Solvation of an Amino Acid: The Appearance of Zwitterionic Structures<sup>†</sup>Martine N. Blom,<sup>‡</sup> Isabelle Compagnon,<sup>‡</sup> Nick C. Polfer,<sup>‡</sup> Gert von Helden,<sup>§</sup> Gerard Meijer,<sup>§</sup> Sándor Suhai,<sup>||</sup> Béla Paizs,<sup>\*,||</sup> and Jos Oomens<sup>\*,‡</sup>*FOM Institute for Plasmaphysics “Rijnhuizen”, Edisonbaan 14, NL-3439 MN Nieuwegein, The Netherlands, Fritz-Haber-Institut der Max-Planck-Gesellschaft, Faradayweg 4-6, D-14195, Germany, and German Cancer Research Center, Im Neuenheimer Feld 580, D-69120 Heidelberg, Germany**Received: January 10, 2007; In Final Form: May 29, 2007*

How many solvent molecules are required to solvate an amino acid? This apparently simple question, which relates to the number of solvent molecules necessary to change the amino acid from its gas-phase neutral structure to the zwitterionic solvated structure, remains unanswered to date. Here we present experimental and theoretical (density functional theory: B3LYP/6-31+G\*\*) infrared spectra for tryptophan–water<sub>*n*</sub> complexes where *n* = 1–6, which suggest that the zwitterionic structure becomes competitive in energy at the high end of the series. Compelling evidence for a gradual transition to zwitterionic structures comes from tryptophan–methanol complexes up to *n* = 9. Starting from *n* = 5, the infrared spectra show increasing intensity in the diagnostic asymmetric COO<sup>−</sup> stretch and in the weaker NH<sub>3</sub><sup>+</sup> bending modes as the cluster size increases. Moreover, convergence toward the Fourier transform infrared spectrum of a solution of tryptophan in methanol is clearly observed. For small solvent complexes (*n* = 1–4), the microsolvation by methanol and water is shown to behave very similarly. A detailed comparison of the experimental and the theoretical spectra allows us to determine both the preferred solvent binding sites on the amino acid and the evolution of conformational structures of tryptophan as the number of attached solvent molecules increases.

## Introduction

Understanding the structure of a biomolecule to predict its function is one of the key challenges facing biology. Because of the immense number of competing intra- and intermolecular forces, this is a highly complex task. By studying small model systems in a controlled simple environment, the influence of the various effects can be assessed individually. The inherent structure of many biomolecules has been determined in the total absence of environmental effects in numerous gas-phase experiments.<sup>1</sup> Comparing these results to solution-phase experiments has shown that the structures can be different,<sup>2</sup> and it leaves one with intriguing questions of what happens in the twilight between isolated molecules and the bulk.<sup>3</sup> In the case of an amino acid, the most spectacular solvent effect is a proton transfer from the acidic group to the amino group resulting in a zwitterion (ZW). Despite being of fundamental interest, the stepwise solvation process, from the isolated molecule to the fully solvated system, remains poorly understood.

To understand the transition from the isolated gas-phase molecule to the molecule in solution, one would like to study partially solvated systems.<sup>4,5</sup> Most microhydration experiments carried out to date involve hydrated ionic systems, where the presence of a metal cation or an added electron disturbs the system to the point where, in the case of an amino acid, the zwitterionic form can be observed even in the absence of solvent molecules.<sup>6–9</sup> Studies on neutral biomolecule–water complexes are mostly carried out in a jet-cooled environment, where, for

instance, the tautomerism in nucleobase–water complexes<sup>10</sup> and in related heterocyclic compounds,<sup>11</sup> as well as singly hydrated monosaccharides,<sup>12</sup> has been investigated. Xu et al.<sup>9</sup> carried out photoelectron spectroscopy on neutral tryptophan–water complexes where they observed only Trp(H<sub>2</sub>O)<sub>*n*</sub><sup>−</sup>, for *n* ≥ 4. This behavior was interpreted as the onset of the zwitterionic structures at *n* = 4 due to an enhanced electron capture for the higher dipole moment ZWs. However, later results by Johnson and co-workers suggested that the preferential formation of particular complexes could also be explained by cluster formation kinetics in the source.<sup>13,14</sup>

Because of the presence of the indole chromophore ring,<sup>15,16</sup> tryptophan is a natural choice for ultraviolet (UV) spectroscopy. The early pioneering UV spectroscopic work on singly hydrated neutral tryptophan was carried out using resonance-enhanced two-photon ionization (R2PI)<sup>17</sup> and laser-induced fluorescence (LIF)<sup>18</sup> spectroscopy. Using infrared (IR) spectroscopy, the ground state vibrational modes of the molecules are probed, which can be compared to density functional theory (DFT) calculations more accurately, thus giving more direct insight into the molecular structure. For instance, the amide I and amide II vibrational bands (around 1500–1700 cm<sup>−1</sup>), corresponding to the C=O stretching and N–H bending modes of the amide linkage, are routinely used to characterize peptides in solution. Recently, IR–UV hole-burning spectra of singly hydrated tryptophan in the 100–1800 cm<sup>−1</sup> spectral range have been reported by Çarçabal et al.<sup>19</sup> and were tentatively interpreted as a superposition of singly, doubly, and triply hydrated tryptophan. In the spectral range 2800–2900 cm<sup>−1</sup>, the IR spectrum of Trp(H<sub>2</sub>O)<sub>1</sub> was explained by the presence of at least two different nonzwitterionic structures.<sup>20</sup> This is consistent with the results of Ebata et al. for Phe(H<sub>2</sub>O)<sub>1</sub>, but for Phe(H<sub>2</sub>O)<sub>2</sub> only one nonzwitterionic structure was observed.<sup>21</sup> The photoelectron

<sup>†</sup> Part of the “Roger E. Miller Memorial Issue”.<sup>\*</sup> To whom correspondence should be addressed. J.O.: E-mail: joso@rijnhuizen.nl; B.P.: E-mail: b.paizs@dkfz-heidelberg.de.<sup>‡</sup> FOM Institute for Plasmaphysics “Rijnhuizen”.<sup>§</sup> Fritz-Haber-Institut der Max-Planck-Gesellschaft.<sup>||</sup> German Cancer Research Center.

spectra of doubly hydrated glycine by Diken et al. indicate the presence of two conformations, but no structural assignment was performed.<sup>14</sup>

Despite their relatively small size, solvated amino acids remain a formidable challenge for theoretical approaches, which is not surprising given the large number of putative conformations connected by low barriers on the potential energy surface. Various computational approaches have been applied to study the solvation process of amino acids, aiming at the question of the number of solvent molecules necessary to energetically stabilize a zwitterionic conformation. The theoretical studies of Snoek et al. on tryptophan–water and of Kassab et al. on glycine–water clusters showed that for three water molecules the zwitterionic and nonzwitterionic species become isoenergetic.<sup>20,22</sup> Tajkhorshid et al. found that at least four water molecules are needed to hydrate the  $\text{NH}_3^+$  and the  $\text{COO}^-$  groups of a zwitterionic alanine.<sup>23</sup>  $\text{Gly}(\text{H}_2\text{O})_6$  was shown to be clearly more stable in the zwitterionic form in calculations on various levels of theory.<sup>24</sup> The hydrogen bond stabilization in the case of methanol is very similar to water, such that analogue structures are expected to be found.<sup>25</sup>

Thus far, the experimental structural information on multiply solvated amino acids is limited, and none of the previous studies, neither theoretical nor experimental, have provided conclusive evidence as to how the structure of an amino acid changes upon solvation and where the neutral-to-zwitterion transition occurs. Here, we present a systematic analysis of the solvation process of a complete series of tryptophan–water ( $\text{Trp}(\text{H}_2\text{O})_{1-6}$ ,  $\text{Trp}(\text{D}_2\text{O})_{1-6}$ ) and tryptophan–methanol complexes ( $\text{Trp}(\text{MeOH})_{1-9}$ ) by means of the IR spectra in the spectral range of  $1300\text{--}1850\text{ cm}^{-1}$ . Using state-of-the-art DFT calculations to interpret them allows us to determine where the preferred binding sites of the solvent are, how the solvent molecules influence the structure of tryptophan, and how many solvent molecules it takes to stabilize a zwitterionic structure. Moreover, the IR spectra of the partially solvated tryptophan complexes are compared to their solution-phase Fourier transform IR (FTIR) spectra to show whether the solution-phase limit is approached.

## Experimental and Theoretical Methods

**Jet-Cooled IR–UV Hole-Burning Spectroscopy.** Experimentally, a distribution of tryptophan–water clusters is formed by Nd:YAG laser desorption of a tryptophan–graphite powder mixture (L-tryptophan: Fluka, Biochemika) from a graphite sample holder positioned directly under the orifice of a pulsed valve (R. M. Jordan Co.). The sample is injected into a moisturized supersonic Argon expansion (with a backing pressure of 3 bar), which is skimmed and then traverses the extraction zone of a time-of-flight mass spectrometer (TOF-MS), where resonant one-color, two-photon ionization is induced using the frequency-doubled output of a pulsed dye laser (R6G, PDL-2). A mass spectrum of the tryptophan–water clusters is shown in Figure 1.

The UV spectra (not shown) appear as broad and structureless bands, except for the  $\text{Trp}(\text{H}_2\text{O})_1$  complex, which shows very broad features as also observed by Snoek et al.<sup>20</sup> The broadening may be due to conformeric heterogeneity, increased temperature as compared to a bare tryptophan in Ar expansion, reduced excited-state lifetimes for the complexes (as observed for protonated tryptophan<sup>26</sup>), congested vibronic bands,<sup>27</sup> or a combination thereof. Nonetheless, the resolution in the IR spectra recorded by IR–UV hole-burning spectroscopy is sufficient to resolve vibrational bands. The IR spectra are

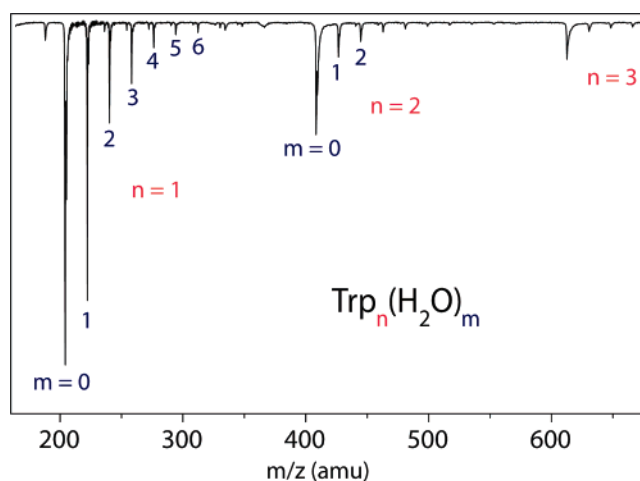


**Figure 1.** Typical time-of-flight mass spectrum of tryptophan–water complexes  $\text{Trp}_n(\text{H}_2\text{O})_m$ .

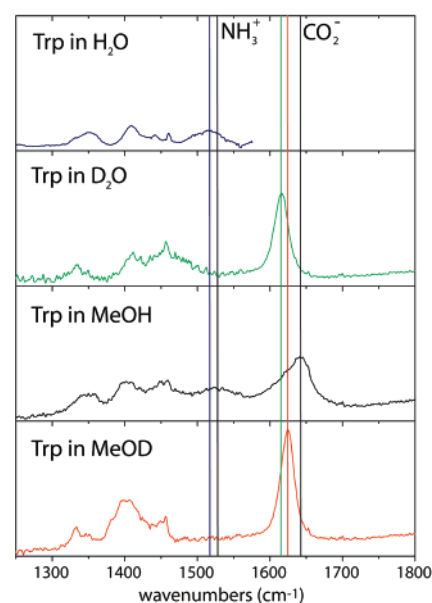


**Figure 2.** FTIR spectra of tryptophan in  $\text{H}_2\text{O}$ ,  $\text{D}_2\text{O}$ , MeOH, and MeOD where the solvent backgrounds spectra have been subtracted. The vertical lines indicate the position of the asymmetric  $\text{CO}_2^-$  stretch for tryptophan in the four different solvents ( $\sim 1630\text{ cm}^{-1}$ ) and the lower-intensity asymmetric bending mode of  $\text{NH}_3^+$  in the nondeuterated solvents ( $\sim 1530\text{ cm}^{-1}$ ). Both of these bands are diagnostic for the presence of the zwitterion in solution. Because of the strong  $\text{H}_2\text{O}$  bending mode absorption around  $1650\text{ cm}^{-1}$ , a reliable difference spectrum could not be obtained for tryptophan in  $\text{H}_2\text{O}$ .

obtained in the mid-IR region ( $1300\text{--}1850\text{ cm}^{-1}$ ) using the free-electron laser (FELIX),<sup>28</sup> which crosses the UV laser in the REMPI extraction zone.<sup>2,16</sup> The UV laser and the pulsed nozzle are run at a 10 Hz repetition rate, whereas FELIX runs at 5 Hz. Hence, a difference signal is generated from alternating shots. This reduces long-term fluctuations in the signal and, moreover, allows us to recognize IR-induced cluster fragmentation, which appears as a negative signal on the product mass channel. Although UV-induced cluster fragmentation has been suggested to occur in some experiments,<sup>19,21,29</sup> it appears to be, at most, a minor effect under our experimental conditions. This is concluded from the observation that each cluster has its own individual IR spectrum (vide infra), and there appears to be little “cross-talk” between the channels. Moreover, from the favorable agreement with the calculations (e.g., from the calculated jump in the energetics between  $n = 3$  and  $n = 4$  and the corresponding

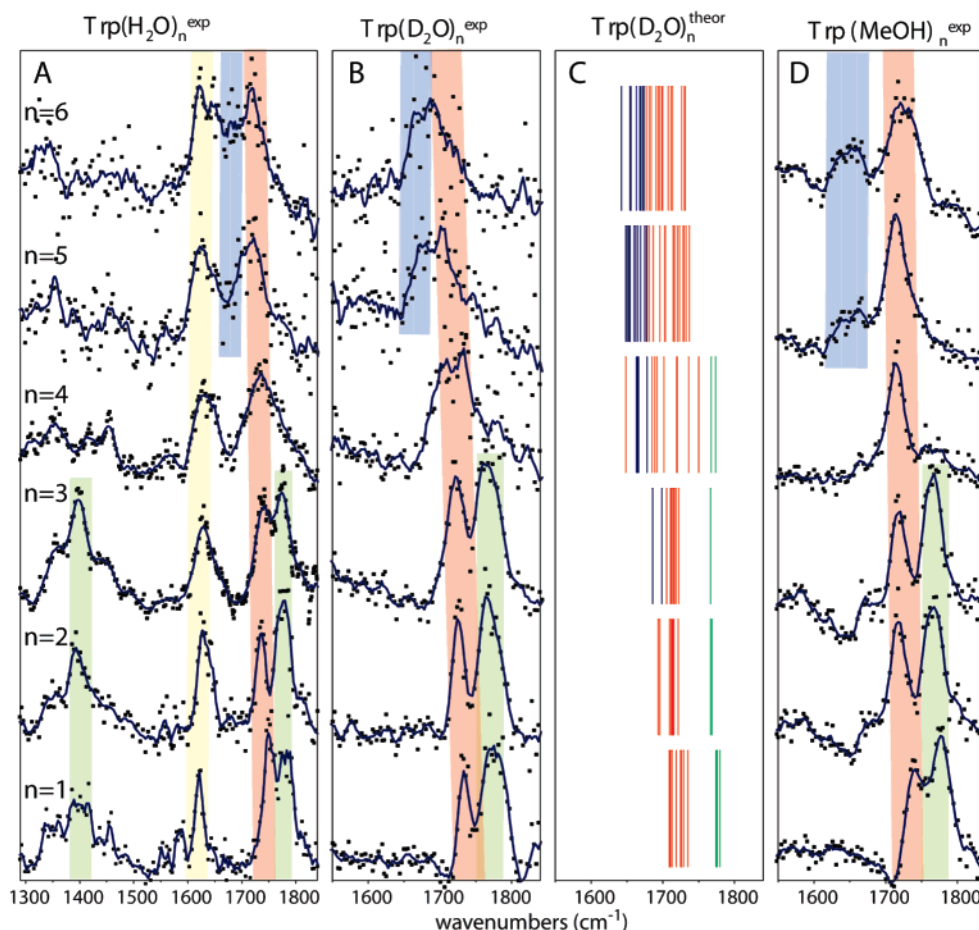


**Figure 3.** Experimental infrared spectra of (A)  $\text{Trp}(\text{H}_2\text{O})_{1-6}$ , (B)  $\text{Trp}(\text{D}_2\text{O})_{1-6}$ , and (D)  $\text{Trp}(\text{MeOH})_{1-6}$  compared to (C) the calculated CO stretching frequencies (scaling factor: 0.987) of  $\text{Trp}(\text{D}_2\text{O})_{1-6}$  for the three distinct structural motifs: zwitterion (ZW, blue) and two nonzwitterionic structures, N1 (red) and N2 (green). The UV excitation frequency is  $34917\text{ cm}^{-1}$  for the  $\text{X}_2\text{O}$  clusters and  $34950\text{ cm}^{-1}$  for the MeOH clusters, although for  $n > 1$  this is not critical (see Figure 5). Structural assignment of the experimental bands is accomplished based on the diagnostic CO stretch ( $1650\text{--}1800\text{ cm}^{-1}$ ) and the C–O–H bending ( $\sim 1400\text{ cm}^{-1}$ ) vibrations. The  $\text{H}_2\text{O}$  bending mode is seen around  $1630\text{ cm}^{-1}$ . For 1–3 water or methanol molecules, the structural families N1 and N2 are both present, whereas at four molecules, the N2 motif disappears. Starting with five solvent molecules, a well separated  $\text{COO}^-$  band is found for  $\text{Trp}(\text{MeOH})_n$ , and a shift of the CO stretch frequency is detected for  $\text{Trp}(\text{H}_2\text{O})_{5-6}$  and  $\text{Trp}(\text{D}_2\text{O})_{5-6}$ , suggesting the appearance of zwitterionic structures.

sudden disappearance of one of the conformers in the experimental spectra (vide infra), the absolute calibration of the number of solvent molecules appears to be correct.

Despite the low intensity of larger clusters in the mass spectrum and the inherently low signal-to-noise ratio in the IR spectra of these species, the reproducibility of the spectra is reasonable. Experiments are repeated for tryptophan– $(\text{D}_2\text{O})_n$  clusters to aid in the spectral interpretation. Note that these experiments were in fact carried out on  $\text{Trp}-d_4(\text{D}_2\text{O})_n$ , where the four hydrogen atoms on the carboxylic acid OH, the amino  $\text{NH}_2$ , and the indole side chain NH of L-tryptophan are exchanged with deuterium atoms to preclude H/D exchange between Trp and  $\text{D}_2\text{O}$ .

**Solution-Phase FTIR Spectroscopy.** The solution-phase experiments were performed with a FTIR spectrometer. Because the solvents show strong absorption bands in the region of interest, a cuvette ( $\text{BaF}_2$ ) with a thickness of  $0.015\text{ mm}$  was used. Spectra were recorded for a  $0.01\text{ M}$  solution of tryptophan in  $\text{H}_2\text{O}$ ,  $\text{D}_2\text{O}$ , MeOH, and MeOD. Solution-phase spectra were generated by subtracting the FTIR spectra of the respective pure solvents.

**Computational Approach.** The conformational spaces of nonzwitterionic and zwitterionic  $\text{Trp}(\text{H}_2\text{O})_n$  ( $n = 1\text{--}6$ ) are extensively probed with the search program recently developed in Heidelberg.<sup>30–32</sup> Cluster geometries and theoretical harmonic

vibrational spectra are obtained at the DFT level (B3LYP/6-31+G\*\*). The complexation energetics are further refined with single point calculations at the BSSE<sup>33–35</sup> corrected second-order Møller–Plesset perturbation theory (MP2) level. The experimental spectra are compared to calculated spectra to allow a structural assignment based on diagnostically important modes: the C=O stretching vibration, in particular.

## Results

**Solution-Phase Spectra.** The solution-phase FTIR spectra of tryptophan in the four different solvents are shown in Figure 2. Note, that the spectrum of tryptophan in  $\text{H}_2\text{O}$  is missing above  $1570\text{ cm}^{-1}$  because of the strong  $\text{H}_2\text{O}$  absorption in this region (see uncorrected solution-phase spectra in Figure S1, Supporting Information), which prevents us from obtaining a reliable difference signal.

The strongest band in these spectra is in the range of  $1616\text{--}1643\text{ cm}^{-1}$  and can be assigned to the asymmetric  $\text{COO}^-$  stretch mode of zwitterionic tryptophan. Note that the  $\text{COO}^-$  stretch band is located at the same position ( $1625\text{ cm}^{-1}$ ) as that observed in FTIR spectra of tryptophan deposited onto a surface using dissolution-spray-deposition.<sup>36</sup> Because of the strong absorption of water in this region, the position of the asymmetric  $\text{COO}^-$  stretch mode in  $\text{H}_2\text{O}$  could not be determined, whereas

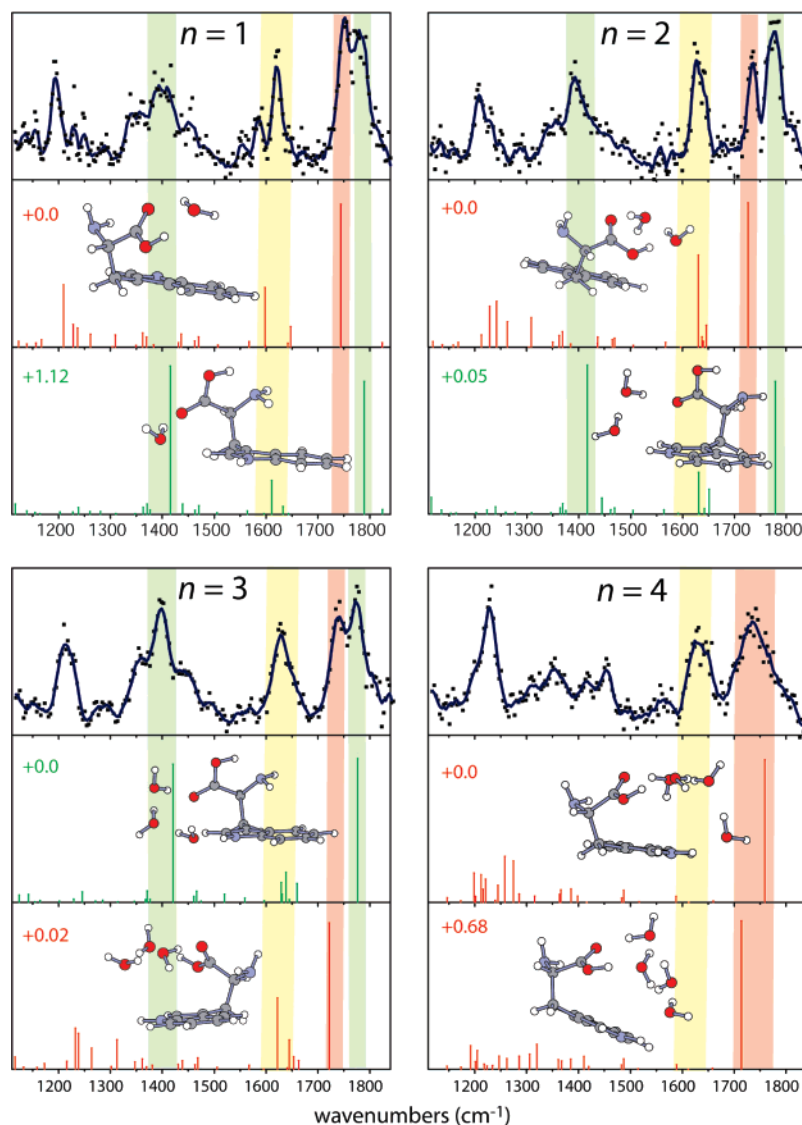


**Figure 4.** IR spectrum of  $\text{Trp}(\text{H}_2\text{O})_{1-4}$  in comparison to the calculated IR frequencies of the nonzwitterionic structures of types N1 and N2 shown with their relative energies  $\Delta E$  [kcal mol $^{-1}$ ]. The structural assignment is indicated by the vertical bars on the CO stretch bands and the COH bending mode (N1, red; N2, green). The  $\text{H}_2\text{O}$  bending mode is observed around 1620  $\text{cm}^{-1}$ .

in  $\text{D}_2\text{O}$  this problem does not arise, although, chemically, the zwitterion is still expected. Upon going from  $\text{D}_2\text{O}$  (1616  $\text{cm}^{-1}$ ) to MeOD (1625  $\text{cm}^{-1}$ ) a slight redshift of 9  $\text{cm}^{-1}$  is observed. This is consistent with the presence of ZWs in methanol as well, given that both are polar solvents with high dielectric constants ( $\epsilon_{\text{H}_2\text{O}} = 80$  and  $\epsilon_{\text{MeOH}} = 33$ ). The CO stretch mode of the nonzwitterionic COOH group is known to be much higher in energy and is found at 1700–1820  $\text{cm}^{-1}$  in various gas-phase experiments.<sup>16</sup> Although the exact position of the asymmetric  $\text{CO}_2^-$  stretch mode depends on the surrounding medium (i.e., vacuum, solvent, or matrix), the difference in frequency to the nonzwitterionic C=O stretch of the COOH group is generally sufficient to distinguish them. In the FTIR spectrum of tryptophan in MeOH, the  $\text{CO}_2^-$  stretch is located at 1643  $\text{cm}^{-1}$ , which enables an estimate of this band in  $\text{H}_2\text{O}$  at 1634  $\text{cm}^{-1}$ , assuming a similar redshift as that observed upon going from MeOD to  $\text{D}_2\text{O}$ .

The asymmetric  $\text{NH}_3^+$  bending around 1530  $\text{cm}^{-1}$  is also indicative of the presence of the zwitterionic structures. Despite its relatively low intensity,<sup>36</sup> the band can clearly be observed in the spectra taken in  $\text{H}_2\text{O}$  and MeOH. The fact that the band is not observed in the spectra of tryptophan in  $\text{D}_2\text{O}$  and MeOD

supports the assignment, as the amino group is deuterated ( $\text{ND}_3^+$ ), thus causing a redshift of the band to below 1200  $\text{cm}^{-1}$ .

**Jet-Cooled Spectra of Tryptophan Water Clusters.** Figure 3 summarizes our experimental and theoretical results for the tryptophan–solvent complexes. The solid line is obtained by applying a five-point adjacent averaging to the experimental datapoints. Columns 3a, 3b, and 3d show the mid-IR spectra of the complexes  $\text{Trp}(\text{H}_2\text{O})_n$ ,  $\text{Trp}(\text{D}_2\text{O})_n$ , and  $\text{Trp}(\text{MeOH})_n$  ( $n = 1 - 6$ ), respectively. The spectra have been recorded with the UV laser tuned to 34 917  $\text{cm}^{-1}$  for  $\text{X}_2\text{O}$  and 34 950  $\text{cm}^{-1}$  for MeOH unless otherwise noted. The calculations predict three distinct structural families: two nonzwitterionic motifs (N1 and N2), as well as the zwitterionic motif. These families can generally be distinguished by their CO stretching frequencies (see Tables 1–6 Supporting Information), which are shown in column 3c for the calculated  $\text{Trp}(\text{D}_2\text{O})_{1-6}$  structures (scaling factor: 0.987, 2 kcal/mol cutoff energy). Structural assignment of the experimental bands to different conformeric families is shown in color-coding and is based on the diagnostic CO stretch (N1, red; N2, green; ZW, blue; 1650–1800  $\text{cm}^{-1}$ ) and C–O–H bending (N2, green;  $\sim 1400$   $\text{cm}^{-1}$ ) vibrations. The water bending mode is observed around 1630  $\text{cm}^{-1}$  and is experimentally

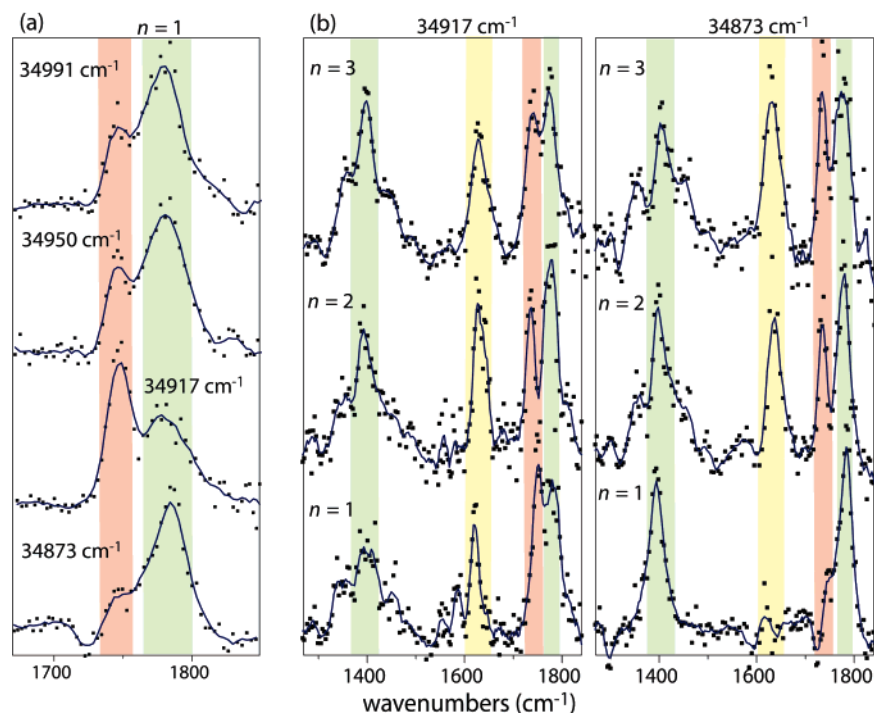


**Figure 5.** (a) IR spectrum of  $\text{Trp}(\text{H}_2\text{O})_1$  at four different UV frequencies. (b) IR spectrum of  $\text{Trp}(\text{H}_2\text{O})_{1-3}$  at two different UV frequencies. The structural assignment is indicated by red (N1) and green (N2) bars on the CO stretch bands and the COH bending mode. The  $\text{H}_2\text{O}$  bending mode is observed around  $1620\text{ cm}^{-1}$ .

assigned using the deuteration experiment. A detailed description of the structures and a thorough analysis of the IR spectra are presented in the following discussion.

The nonzwitterionic motifs (N1 and N2) differ structurally in that a hydrogen bond is formed between the amino H-atoms and the acidic O-atom in N1, whereas in the N2 motif a hydrogen bond is formed between the acidic H-atom and the amino N-atom (see structures in Figure 4). This results in a red-shifted CO stretch frequency in the case of N1 relative to N2 and in an intense COH bending mode for N2. Previous studies have shown that five distinguishable conformers can be identified for bare tryptophan, three of which can be considered as N1 and two, including the lowest energy conformer, as N2.<sup>16,36</sup>

The experimental spectra of  $\text{Trp}(\text{H}_2\text{O})_{1-4}$  and the lowest energy N1 and N2 conformers are presented in detail in Figure 4. For  $\text{Trp}(\text{H}_2\text{O})_1$ , two distinct bands can be observed in the range where the C=O stretching bands are expected ( $1700\text{--}1800\text{ cm}^{-1}$ ), and both agree well with the predicted C=O frequencies for the nonzwitterionic families N1 and N2. Further proof for this assignment is given by the COH bending mode ( $1400\text{ cm}^{-1}$ ), which is diagnostic for the presence of N2. In both structural motifs, the acid group of tryptophan is the preferred site of water binding. For the N1 structural family, the water molecule binds through hydrogen bonds to the C=O and the OH groups, thereby forming a six-membered ring structure. Conversely, in N2 structures, water attachment exclusively occurs on the C=O group, as the OH group is already H-bonded to the amino group, thereby giving rise to the intense COH bending mode at  $\sim 1400\text{ cm}^{-1}$ .

In a previous study on hydrated tryptophan by Çarçabal et al.,<sup>19</sup> the N2 structural family was not observed, despite the clear evidence for N2 in the present experiment. Because they were also not able to observe intact multiply hydrated tryptophan we suspect that this may be due to different cluster formation conditions and/or UV selection. In the experiments by Ebata et

al. on hydrated phenylalanine, the N2 structure was also not found.<sup>21</sup> Our calculations show that, in the case of the tryptophan–water complexes, the N2 structures are stabilized by the bonding of water molecules to the hydrogen of the indole NH group, which is not possible for phenylalanine. Water is known to function as an H-acceptor of the NH group on the indole ring, as has been reported for indole–water complexes.<sup>38,39</sup>

Further evidence for the coexistence of two distinct conformeric families comes from the ion-dip spectra recorded at different UV excitation wavelengths. Despite the broad and unresolved bands in the UV spectra, some structure is still observed for  $\text{Trp}(\text{H}_2\text{O})_1$ , and separate IR/UV ion-dip spectra were recorded with the UV laser set to  $34\,991$ ,  $34\,950$ ,  $34\,917$ , and  $34\,873\text{ cm}^{-1}$ , as shown in Figure 5. Clear differences in the conformer distribution are detected depending on the UV wavelength used. At  $34\,917\text{ cm}^{-1}$ , structures belonging to the N1 motif are dominant, whereas at  $34\,873\text{ cm}^{-1}$  only N2 structural family conformers are detected. This partial UV selectivity is lost for bigger cluster sizes, and essentially identical IR ion-dip spectra are generated for  $\text{Trp}(\text{H}_2\text{O})_2$  and  $\text{Trp}(\text{H}_2\text{O})_3$ , as shown in Figure 5b and as also observed by Çarçabal et al.<sup>19</sup> This is found to also be the case for larger clusters as well as for the other solvent molecules, despite several attempts to find IR spectral differences by tuning the UV laser to a different wavelength within the unresolved excitation spectrum.

For  $\text{Trp}(\text{H}_2\text{O})_2$ , the C=O stretching modes of both N1 and N2 are slightly red-shifted as compared to  $\text{Trp}(\text{H}_2\text{O})_1$ , whereas for  $\text{Trp}(\text{H}_2\text{O})_3$ , no further red-shift takes place (see Figure 3). This trend is well predicted by the calculations. The attachment of a second and a third water molecule to N1 results in the formation of an 8-membered and then a 10-membered ring. In the case of N2, the additional water molecules form a bridge between the C=O group and the indole NH. Although the C=O stretching frequencies of the zwitterionic structures are comparable to those of the N1 motif for 1–2 water molecules,

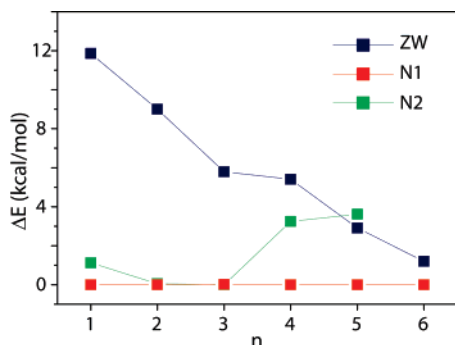


**Figure 6.** Computed relative MP2 energies of the lowest-energy structures versus the number of water molecules ( $n$ ) for each of the three structural motifs: nonzwitterionic structures N1 and N2 and the zwitterionic (ZW) structure. The values are corrected for zero point energy (ZPE), and relative stabilities are the same for  $\text{H}_2\text{O}$  and  $\text{D}_2\text{O}$  clusters. The structural families N1 and N2 are thus predicted to exist for  $\text{Trp}(\text{X}_2\text{O})_n$ , for  $n = 1-3$ , whereas at  $n \geq 4$  water molecules, N2 should disappear. This is confirmed experimentally. The energy gap between the best ZW and nonzwitterionic structures gradually closes as more water molecules are added. At 5–6 water molecules the ZW starts becoming energetically available, thus mirroring the appearance of the ZW in the experimental spectrum.

the calculations predict a significantly lower frequency for 3 water molecules (tables with CO stretching frequencies and relative energies for larger complexes are given in Tables S1–3, Supporting Information). Experimentally, no zwitterionic structures are observed for  $\text{Trp}(\text{H}_2\text{O})_3$ , which, in combination with the computed thermochemistry (see Figure 6), makes it unlikely that a zwitterion motif would occur for  $n = 1, 2$ .

With the addition of a fourth water molecule there is a sudden disappearance of both the COH bend (at  $1400\text{ cm}^{-1}$ ) and the higher-frequency C=O stretch associated with the N2 structure. This structure does not appear in the larger complexes either, which is in agreement with calculated energetics for the N2 structures, which happen to become much less favorable than N1 for  $n \geq 4$  (Figure 6). This suggests a “sea change” in the energetics as one goes from three to four water molecules, which is somewhat surprising given that both the N1 and the N2

structures were found to be very close in energy up to  $\text{Trp}(\text{H}_2\text{O})_3$ . As the N2 family disappears, there is also a significant broadening of the C=O stretching band assigned to the N1 family as compared to the smaller complexes. This is mirrored in the large increase in the number of substructures found within the N1 family, resulting in an extended range of the calculated C=O stretching frequencies for N1 (Figure 3c). For these complexes, interpretation of the  $\text{Trp}(\text{H}_2\text{O})_n$  spectra is complicated by the presence of the  $\text{H}_2\text{O}$  bending modes, which increasingly overlap with the C=O stretching band. Moreover, mode coupling between the  $\text{H}_2\text{O}$  bending modes and the C=O stretching mode appear to cause substantial discrepancies between computed and experimental spectra, as is observed for  $\text{Trp}(\text{H}_2\text{O})_4$  in Figure 4. These problems can be circumvented by analyzing the  $\text{Trp}(\text{D}_2\text{O})_n$  IR spectra, where the water bending mode is shifted to around  $1200\text{ cm}^{-1}$  (see Figure 7, outside the range plotted in Figure 3).

In Figure 7, a detailed comparison between the experimental spectra for  $\text{Trp}(\text{D}_2\text{O})_{4-6}$  and the calculated spectra for the lowest energy N1 and ZW species is shown. Up to four water molecules, the calculated energies of the zwitterionic structures are very high, as shown in Figure 6, thereby precluding their existence. However, note that the presence of a small amount of ZW conformers for four water molecules, as suggested by Xu et al.,<sup>9</sup> cannot be completely excluded experimentally, although the nonzwitterionic structure is clearly dominant. For larger complexes, the energy gap between zwitterionic and nonzwitterionic structures begins to close (see Figure 6), making the zwitterions energetically available. The DFT calculations for the deuterated complexes clearly show that the CO stretching frequencies of the zwitterionic structures are lower than those for the nonzwitterionic structures.

Upon going to five and six water molecules (Figure 7), the CO stretching band is significantly red-shifted from  $\sim 1720$  to  $1690\text{ cm}^{-1}$ . Because there is no shift of the CO stretch band between  $n = 2-4$ , this shift could be rationalized by the appearance of the zwitterion. In fact, the observed shoulder to lower frequencies reasonably matches with the calculated CO frequencies of the zwitterionic structures. Nonetheless, it is

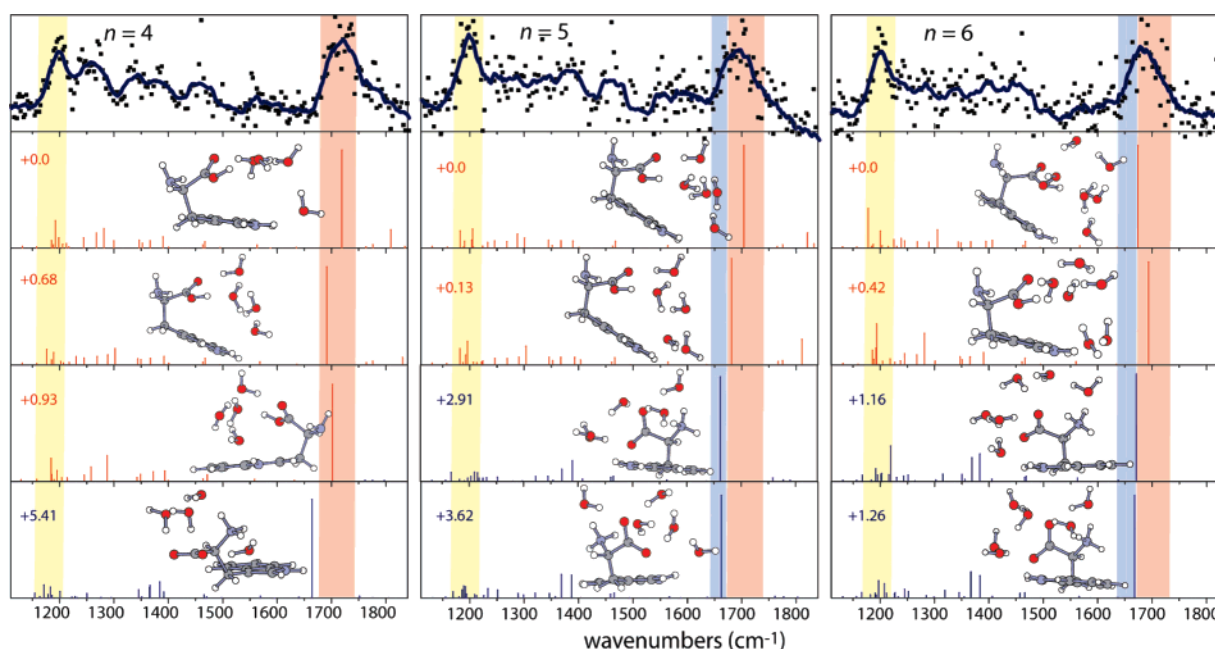


**Figure 7.** IR spectrum of  $\text{Trp}(\text{D}_2\text{O})_{4-6}$  in comparison to the calculated IR frequencies of the different zwitterionic and nonzwitterionic structures shown with their relative energies in  $\text{kcal mol}^{-1}$ . The structural assignment is indicated by color-coding of the CO stretch bands in the experimental spectrum (zwitterionic, dark blue; nonzwitterionic, red). The  $\text{D}_2\text{O}$  bending mode around  $1200\text{ cm}^{-1}$  is depicted in yellow.

speculative to assign this shoulder as such (as we have done here), given the low signal-to-noise ratios of the bands and the fact that no two resolvable bands are observed.

The calculated energy gap for five attached water molecules (2.9 kcal/mol, see Figure 6) would not rationalize the observation of zwitterionic conformers, but at six water molecules, an observable fraction of the population would be expected to be in the zwitterionic form based on the thermochemistry. It is clear that additional water attachment will make the zwitterionic structure progressively more favorable, eventually leading to the total disappearance of the nonzwitterionic structure in an aqueous environment. At six water molecules this process is certainly not completed yet, as only a minor proportion of the structures appears to be in the zwitterionic form. For the zwitterionic Trp(D<sub>2</sub>O)<sub>6</sub> complexes, we experimentally and theoretically determined the position of the COO<sup>-</sup> stretch frequency to be at about 1665 cm<sup>-1</sup>, which is still significantly different from the position of this band in the solution-phase FTIR spectrum (1616 cm<sup>-1</sup>). Indeed, the computed structures for six water molecules show that the important functional groups of the zwitterionic structures (i.e., COO<sup>-</sup> and NH<sub>3</sub><sup>+</sup>) are only partially solvated, and thus further solvent stabilization and weakening of the CO<sub>2</sub><sup>-</sup> bond can take place. Calculations have also shown that the relative energy of zwitterionic structures in solution is further lowered because of dielectric stabilization by the solvent.<sup>24</sup> Hence, it is clear that the present experimental data do not give a conclusive answer as to where zwitterionic structures truly start to appear, and it is unfortunate that no larger complexes could be generated experimentally. For Trp(MeOH)<sub>n</sub> complexes, on the other hand, it was possible to generate complexes up to *n* = 9, and this has enabled us to obtain a clearer picture on this question.

**Tryptophan–Methanol Clusters.** The series of IR ion-dip spectra for tryptophan–methanol clusters up to *n* = 9 is shown in Figure 8. Although high-level calculations are not available for the methanol clusters, the experimental data are of interest because they allow us to observe the solvation trends out to cluster sizes larger than tryptophan–water complexes. As for the D<sub>2</sub>O complexes, the band due to the H<sub>2</sub>O bending mode near 1640 cm<sup>-1</sup> that could obscure a zwitterionic CO<sub>2</sub><sup>-</sup> stretching mode is not present in MeOH. Instead, a strong vibrational band of methanol (OH bend, CH<sub>3</sub> deformation), growing in intensity with *n*, is observed at 1460 cm<sup>-1</sup>, well outside the range of interest here. It is therefore not necessary to use deuterated methanol for these experiments.

For the smaller clusters (*n* = 1–4), a behavior almost identical to that of the water clusters is observed; two conformeric families are present for *n* = 1–3, and upon addition of the fourth methanol, one of the two conformers (N2) suddenly disappears. Apparently, the solvation dynamics in water and methanol are very similar, which is not surprising given their similar structures and their high dielectric constants ( $\epsilon_{\text{H}_2\text{O}} = 80$ ,  $\epsilon_{\text{MeOH}} = 33$ ), which was also found in the computations by Paxton et al.<sup>25</sup>

The relatively narrow C=O stretch band and the better signal-to-noise ratio in the tryptophan–methanol complex spectra enable us to resolve the nonzwitterionic CO stretch and the zwitterionic asymmetric CO<sub>2</sub><sup>-</sup> stretch band as separate bands, whereas this was not possible for the tryptophan–water complexes (see Figure 3). The latter band starts to grow at Trp(MeOH)<sub>5</sub> and increases in relative intensity as *n* increases. At the same time, the relative intensity of the C=O stretching band of the nonzwitterionic COOH group gradually fades.

The top panel of Figure 8 shows the FTIR spectrum of tryptophan in methanol as the solution-phase limit. The fre-

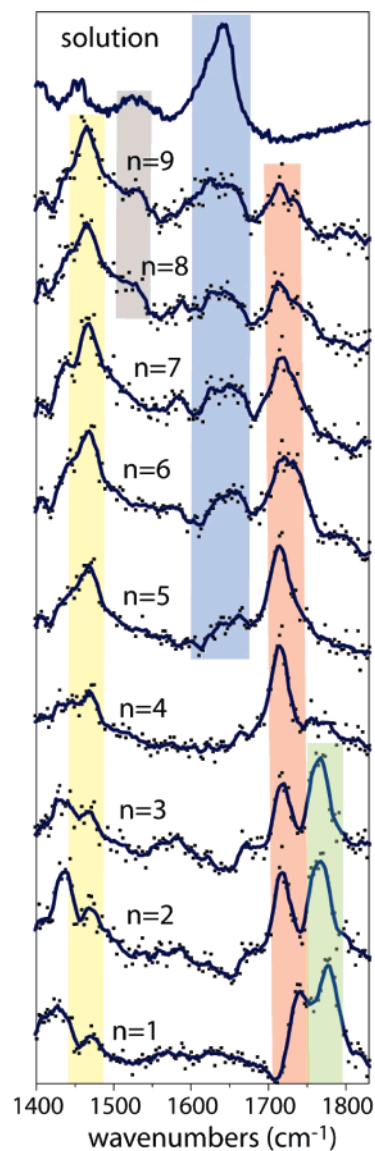


**Figure 8.** Experimental infrared spectra of Trp(MeOH)<sub>1–9</sub> and tryptophan in methanol solution (*n* → ∞). Structural assignment of the experimental bands is indicated by color-coding and is based on the diagnostic C=O stretch (two nonzwitterionic structures N1 (red) and N2 (green): 1690–1800 cm<sup>-1</sup>), the CO<sub>2</sub><sup>-</sup> stretch, and the NH<sub>3</sub><sup>+</sup> bend (zwitterionic structures, CO<sub>2</sub><sup>-</sup> (blue): 1650 cm<sup>-1</sup>, NH<sub>3</sub><sup>+</sup> (gray): 1520 cm<sup>-1</sup>). The vibrational band of methanol (OH bend, CH<sub>3</sub> deformation) is highlighted in yellow.

quency of the zwitterionic Trp(MeOH)<sub>5–9</sub> clusters gives a close match with that of the zwitterionic tryptophan in solution (1643 cm<sup>-1</sup>), thus providing strong evidence for the gradual transition to zwitterionic structures. Note that this is not the case for the position of the stretch frequency of zwitterionic tryptophan in water, which is at about 1665 cm<sup>-1</sup> for Trp(D<sub>2</sub>O)<sub>6</sub> and at 1616 cm<sup>-1</sup> in the D<sub>2</sub>O solution. It is likely that, in the case of the more polar water, the O–C–O<sup>-</sup> bonds are further weakened by the additional water molecules, thereby resulting in a further shift of the asymmetric COO<sup>-</sup> stretch to lower wavenumbers, as is seen for tryptophan in the aqueous solution.

Further evidence for the appearance of zwitterionic structures for the tryptophan–methanol experiments is given by the lower intensity asymmetric NH<sub>3</sub><sup>+</sup> bend. In solution this band is located at 1530 cm<sup>-1</sup> (see Figure 2 and the top panel of Figure 8).<sup>37</sup> Similarly, in the gas-phase measurements, progressively more absorption is observed at this position, starting with Trp(MeOH)<sub>5</sub>

and resulting in a weak but clearly discernible  $\text{NH}_3^+$  bending band for  $\text{Trp}(\text{MeOH})_{8-9}$ . Thus, the increasing fraction of zwitterionic structures as  $n$  increases is further evidenced by the growing asymmetric  $\text{NH}_3^+$  bending band. For the tryptophan–water clusters, this band cannot be recognized because of the low ion signal for larger clusters.

## Conclusions

Using IR spectroscopy and DFT calculations, we present consistent evidence that water preferentially binds to the carboxylic acid group and that the interaction with the water molecules strongly affects the relative energetics of different structural motifs. Theoretical and experimental spectra are in close agreement for  $\text{Trp}(\text{water})_{1-4}$ , thus providing a true benchmark result for sequential hydration. The uniqueness of the IR spectra for each  $n$ , combined with the good agreement with calculations, indicates that little or no UV fragmentation occurs under our experimental conditions. Small solvated complexes, with up to three solvent molecules, are found to be nonzwitterionic and exhibit two distinct conformeric motifs. Upon the addition of one more solvent molecule, one of these motifs disappears, but the ZW is not observed. The solvation dynamics of methanol shows exactly the same trends as water over this range. The question of where the transition to zwitterionic structures occurs is difficult to answer based on the tryptophan–water complexes alone. Nonetheless, the tryptophan–methanol complexes show convincing evidence that a minimum of five solvent molecules are necessary to observe a zwitterionic structure, based on the appearance of the diagnostic  $\text{CO}_2^-$  band. This suggests that the observed red-shift for  $\text{Trp}(\text{H}_2\text{O})_{5-6}$  is also due to the presence of ZWs, as predicted by the calculations. Water should, in principle, be better at stabilizing ZWs, given that it is the more polar solvent. An important difference in the IR spectra for water and methanol at 5–6 solvent molecules lies in the fact that the zwitterionic and nonzwitterionic CO stretch bands are clearly separated in the case of methanol, whereas this is not the case for water. Moreover, for  $\text{Trp}(\text{H}_2\text{O})_5$  this band is still blue-shifted  $50\text{ cm}^{-1}$  more than in solution, and this renders the interpretation much more difficult. The IR spectra for the  $\text{Trp}(\text{MeOH})_{1-9}$  complexes, on the other hand, are seen to converge progressively to the bulk solution-phase spectrum, both for the  $\text{CO}_2^-$  as well as for the  $\text{NH}_3^+$  vibrations. In our experiment, the transition from nonzwitterionic to zwitterionic structures occurs very gradually, and the exact number of solvent molecules required to form the ZW is hence not clearly defined. The solvation process is still not completed at nine solvent molecules as a mixture of zwitterionic and nonzwitterionic structures is observed.

**Acknowledgment.** This work is part of the research program of FOM, which is financially supported by the Nederlandse Organisatie voor Wetenschappelijk Onderzoek (NWO). The assistance by the FELIX staff, in particular B. Redlich and A. F. G. van der Meer, is gratefully acknowledged.

**Supporting Information Available:** FTIR spectra of Trp solutions before subtraction of solvent contribution. Computed energies and CO stretch frequencies of all optimized structures for  $\text{Trp}(\text{water})_n$  for  $n = 1-6$ . This material is available free of charge via the Internet at <http://pubs.acs.org>.

## References and Notes

- (1) Special issue “Bioactive Molecules in the Gas Phase” *Phys. Chem. Chem. Phys.* **2004**, *6*, 2543–2890.
- (2) Compagnon, I.; Oomens, J.; Meijer, G.; von Helden, G. *J. Am. Chem. Soc.* **2006**, *128*, 3592–3597.
- (3) Brauman, J. I. *Science* **1996**, *271*, 889.
- (4) Jarrold, M. F. *Annu. Rev. Phys. Chem.* **2000**, *51*, 189.
- (5) Zwier, T. S. *Annu. Rev. Phys. Chem.* **1996**, *47*, 205.
- (6) Kapota, C.; Lemaire, J.; Maitre, P.; Ohanessian, G. *J. Am. Chem. Soc.* **2004**, *126*, 6485.
- (7) (a) Polfer, N. C.; Paizs, B.; Snoek, L. C.; Compagnon, I.; Suhai, S.; Meijer, G.; von Helden, G.; Oomens, J. *J. Am. Chem. Soc.* **2005**, *127*, 8571. (b) Polfer, N. C.; Dunbar, R. C.; Oomens, J. *J. Am. Soc. Mass Spectrom.* **2007**, *18*, 512.
- (8) (a) Kamariotis, A.; Boyarkin, O. V.; Mercier, S. R.; Beck, R. D.; Bush, M. F.; Williams, E. R.; Rizzo, T. R. *J. Am. Chem. Soc.* **2006**, *128*, 905–916. (b) Bush, M. F.; O’Brien, J. T.; Prell, J. S.; Saykally, R. J.; Williams, E. R. *J. Am. Chem. Soc.* **2007**, *129*, 1612–1622.
- (9) Xu, S.; Nilles, J. M.; Bowen, K. H. *J. Chem. Phys.* **2003**, *119*, 10696.
- (10) Abo-Riziq, A.; Crews, B.; Grace, L.; de Vries, M. S. *J. Am. Chem. Soc.* **2005**, *127*, 2374.
- (11) Tanner, C.; Thut, M.; Steinlin, A.; Manca, C.; Leutwyler, S. *J. Phys. Chem. A* **2006**, *110*, 1758.
- (12) Çarçabal, P.; Jockusch, R. A.; Hünig, I.; Snoek, L. C.; Kroemer, R. T.; Davis, B. G.; Gamblin, D. P.; Compagnon, I.; Oomens, J.; Simons, J. P. *J. Am. Chem. Soc.* **2005**, *127*, 11414.
- (13) Diken, E. G.; Hammer, N. I.; Johnson, M. A. *J. Chem. Phys.* **2004**, *120*, 9889.
- (14) Diken, E. G.; Headrick, J. M.; Johnson, M. A. *J. Chem. Phys.* **2005**, *122*, 224317.
- (15) Rizzo, T. R.; Park, Y. D.; Levy, D. H. *J. Chem. Phys.* **1986**, *85*, 6945–6951.
- (16) Bakker, J. M.; McAleese, L. M.; Meijer, G.; von Helden, G. *Phys. Rev. Lett.* **2003**, *91*, 203003.
- (17) Peteanu, L. A.; Levy, D. H. *J. Phys. Chem.* **1988**, *92*, 6554.
- (18) Teh, C. K.; Sipiør, J.; Sulkes, M. *J. Phys. Chem.* **1989**, *93*, 5393.
- (19) Çarçabal, P.; Kroemer, R. T.; Snoek, L. C.; Simons, J. P.; Bakker, J. M.; Compagnon, I.; Meijer, G.; Helden, G. *Phys. Chem. Chem. Phys.* **2004**, *6*, 4546.
- (20) Snoek, L. C.; Kroemer, R. T.; Simons, J. P. *Phys. Chem. Chem. Phys.* **2002**, *4*, 2130.
- (21) Ebata, T.; Hashimoto, T.; Ito, T.; Inokuchi, Y.; Altunsoy, F.; Brutschy, B.; Tarakeshwar, P. *Phys. Chem. Chem. Phys.* **2006**, *8*, 4783–4791.
- (22) Kassab, E.; Langlet, J.; Evleth, E.; Akacem, Y. *Theochem* **2000**, *531*, 267–282.
- (23) Tajkhorshid, E.; Jalkanen, K. J.; Suhai, S. *J. Phys. Chem. B* **1998**, *102*, 5899–5913.
- (24) Fernandez-Ramos, A.; Smedarchina, Z.; Siebrand, W.; Zgierki, M. *Z. J. Chem. Phys.* **2000**, *113*, 9714.
- (25) Paxton, A. T.; Harper, J. B. *Mol. Phys.* **2004**, *102*, 953–958.
- (26) Boyarkin, O. V.; Mercier, S. R.; Kamariotis, A.; Rizzo, T. R. *J. Am. Chem. Soc.* **2006**, *128*, 2816–2817.
- (27) Watanabe, T.; Ebata, T.; Tanabe, S.; Mikami, N. *J. Chem. Phys.* **1996**, *105*, 408–419.
- (28) Oepts, D.; van der Meer, A. F. G.; van Amersfoort, P. W. *Infrared Phys. Technol.* **1995**, *36*, 297.
- (29) Lee, K. T.; Sung, J.; Lee, K. J.; Kim, S. K.; Park, Y. D. *J. Chem. Phys.* **2002**, *116*, 8251.
- (30) Paizs, B.; Suhai, S. *Mass Spectrom. Rev.* **2005**, *24*, 508.
- (31) Paizs, B.; Suhai, S. *J. Am. Soc. Mass Spectrom.* **2004**, *15*, 103.
- (32) Wyttenbach, T.; Paizs, B.; Barran, P.; Brecci, L.; Liu, D.; Suhai, S.; Wysocki, V. H.; Bowers, M. T. *J. Am. Chem. Soc.* **2003**, *125*, 13768.
- (33) Boys, S. B.; Bernardi, F. *Mol. Phys.* **1970**, *19*, 553.
- (34) Paizs, B.; Suhai, S. *J. Comput. Chem.* **1998**, *19*, 575.
- (35) Salvador, P.; Paizs, B.; Duran, M.; Suhai, S. *J. Comput. Chem.* **2001**, *22*, 765.
- (36) Snoek, L. C.; Kroemer, R. T.; Hockridge, M. R.; Simons, J. P. *Phys. Chem. Chem. Phys.* **2001**, *3*, 1819–1826.
- (37) Cao, X.; Fischer, G. *J. Phys. Chem. A* **1999**, *103*, 9995–10003.
- (38) Tubergen, M. J.; Levy, D. H. *J. Phys. Chem.* **1991**, *95*, 2175–2181.
- (39) Carney, J. R.; Hagemester, F. C.; Zwier, T. S. *J. Chem. Phys.* **1998**, *108*, 3379–3382.